

# Model Vulnerability to Distributional Shifts over Image Transformation Sets

Riccardo Volpi<sup>1</sup>, Vittorio Murino<sup>1,2</sup>  
 {riccardo.volpi,vittorio.murino}@iit.it

<sup>1</sup>Istituto Italiano di Tecnologia

<sup>2</sup>Università di Verona

## Abstract

We are concerned with the vulnerability of computer vision models to distributional shifts. We cast this problem in terms of combinatorial optimization, evaluating the regions in the input space where a (black-box) model is more vulnerable. This is carried out by combining image transformations from a given set and standard search algorithms. We embed this idea in a training procedure, where we define new data augmentation rules over iterations, accordingly to the image transformations that the current model is most vulnerable to. An empirical evaluation on classification and semantic segmentation problems suggests that the devised algorithm allows to train models more robust against content-preserving image transformations, and in general, against distributional shifts<sup>1</sup>.

## 1. Introduction

When designing a machine learning system, we generally desire it may perform well on a wide realm of different domains. However, typically, the training data at disposal is defined by samples from a limited number of distributions, resulting in unsatisfactory performance when the model will have to process data from unseen distributions [24, 9, 7, 50]. This problem is typically referred to as *distributional shift* or *domain shift*, and it was shown to affect models even in cases where the shift between training and testing domain is – apparently – very little [43, 44].

Such vulnerability also affects the robustness of machine learning models against input manipulations [17, 22, 23], potentially creating harmful situations. As a concrete example, consider the algorithms that analyze images uploaded to social networks in order to evaluate, *e.g.*, if an image contains violence or adult content. The huge set of image modifications that users might carry out can make the underlying learning systems fail in several ways if they, acci-



Figure 1. (Top) Image subdivided in two parts. The left one is not modified; the right one was subject to a content-preserving transformation. Image transformations can cause distributional shifts that models are not able to handle (bottom-left). Models trained with the methods proposed in this paper are more robust against a variety of transformations (bottom-right).

dentally or with malicious intent, cause a *shift* that the models are not able to figure out. Recognizing this weakness of modern learning systems, an important research direction is defining methods to understand *a priori* which distributional shifts will lead to a fail of the model.

In this paper, we start from this idea, and develop methods to evaluate and improve the performance of machine learning models for vision tasks, when the input can be modified through a series of content-preserving image transformations. With *content-preserving*, we mean transformations that do not modify an image content, but only the way it is portrayed (*e.g.*, modifying RGB intensities, enhancing contrast, applying filters, etc) [17].

We cast this problem in terms of combinatorial optimization. Given a black-box model, a bunch of samples, and a set of image transformations, our goal is to individuate the distributional shifts that the model is most vulnerable to when image transformation tuples (namely, concatenations of transformations) are applied. To find these tuples, we investigate two different search algorithms – random search and evolution-based search – showing that it is easy to find tuples that severely deteriorate the model performance for

<sup>1</sup>Code at [github.com/ricvolpi/domain-shift-robustness](https://github.com/ricvolpi/domain-shift-robustness)

a variety of tasks, such as face detection, semantic scene segmentation, and classification. The main application for this method as-is, is to evaluate the vulnerability of a machine learning model *before* its deployment. Coupled with proper transformation sets, this tool can indeed be used to verify the robustness of a model under a broad variety of input manipulations and visual conditions.

Furthermore, we introduce a training procedure to learn more robust models against this class of transformations. We design an algorithm where new data augmentation rules are included over iterations, in order to cover the distributional shifts where the current model is more vulnerable. We show that models trained in this way are more robust against content-preserving image manipulations and, moreover, better generalize to unseen scenarios at test time.

### 1.1. Background and related work

**Vulnerability of learning systems.** Recently, the vulnerability of learning systems in different scenarios has gained a lot of attention. A widely studied area is the one related to defense against adversarial perturbations. Gilmer et al. [17] makes a distinction between perturbations that are merely *content-preserving* or *indistinguishable*. The latter case takes into account imperceptible (to human eye) input perturbations that make a model fail. This paradigm has been extensively studied in a substantial body of works [18, 47, 29, 20, 38, 35].

The case of content-preserving transformations instead takes into account a broader range of transformations. Given some input, the content-preserving transformations are the ones that do not change its content, even if the appearance may change significantly. For example, Gilmer et al. [17] explore the performance of a classifier trained on MNIST [28] when the input is modified by altering the background or adding random lines. Brown et al. [11] show that we can cause model failure by including adversarial patches in an image. Hosseini et al. [22] realize that ConvNets are vulnerable to negative images. The same research group, in an other work [23], shows that we can find hue and saturation shifts for a given image that a model is vulnerable to. Furthermore, recent works [21, 16] discover that state-of-the-art ImageNet models are vulnerable towards simple image modifications. In particular, Hendrycks et al. [21] have found that these models are not resistant towards simple noise sources, and Geirhos et al. [16] have shown that these models are biased towards the texture of the objects.

As stated by Gilmer et al. [17], we also deem that “*the space of content-preserving image transformations remains largely unexplored in the literature*”. One of the aims of this work is to help filling this gap, proposing methods to study, generate, and be robust against content-preserving image transformations. Differently from previous works

(e.g., [23]), we are not interested in finding adversarial transformations for *single* images. We are instead interested in discovering the distributional shifts that a model is *in general* more vulnerable, applying the same transformation to all the images in the provided set. In this sense, this work is related to Moosavi-Dezfooli et al. [38], where a single *imperceptible* perturbation that fools ImageNet models is found.

**Robustness against distributional shifts.** There is a significant body of works whose goal is overcoming issues related to distributional shifts. One of the main research direction is *domain adaptation* [24, 9, 45, 15, 51, 48, 39, 52], where the goal is better generalizing to domains of interest for which only unlabeled data are available. While there are algorithms that solve this task with remarkable results across a variety of tasks, the assumption of an *a priori* fixed target distribution is often too strong.

In *domain generalization* [30, 40, 41, 46, 36, 53, 31, 33, 53] the problem of dealing with unseen distributions is coped. Usually, the proposed algorithms start from the assumption that the training dataset comprises a number of different populations. One exception is the method proposed in [53], where the authors introduce a worst-case formulation that improves generalization performance across distributions close to the training one in the semantic space, using a single-source distribution as starting point.

Tobin et al. [49] introduce *domain randomization* for models trained through simulated data. It generates a randomized variety of visual conditions during training, hoping to better generalize when testing with real data.

In this context, the method devised in [53] is the most related approach to the training procedures detailed in Section 4, since they are aimed at learning models that better generalize to unseen scenarios, without any assumption on the number of data populations in the training set. As results will show, the training procedure proposed in [53] is only slightly more resistant than the Empirical Risk Minimization (ERM) baseline against the transformations we will present in Section 3, and significantly less performing than models trained through the training algorithm proposed in this work in domain generalization settings.

## 2. Problem formulation

Let  $\mathbb{M}(\cdot)$  be a model that takes in input images and provides an output accordingly to the given task. Let  $D = \{(x^{(i)}, y^{(i)})\}_{i=0}^m \sim P(X, Y)$  be a set of datapoints with their labeling, drawn from some data distribution. Finally, let  $\mathbb{T} = \{(\tau^{(i)}, l_i^{(j)}), i = 1 \dots N_T, j = 1 \dots N_i\}$  be a finite set, where each object  $t = (\tau^{(i)}, l_i^{(j)})$  is a data transformation  $\tau$  with a related magnitude  $l$ . The transformations give in output datapoints in the same format as the input ones

(RGB images throughout this work)<sup>2</sup>. The transformations can be concatenated and repetitions are allowed; we define a composite transformations as a transformation tuple. We define the set of all the possible transformation tuples that one can obtain by combining objects in  $\mathbb{T}$  as

$$\mathbb{T}_N = \{\text{all } N\text{-tuples from } \mathbb{T}\} \quad (1)$$

A tuple  $T \in \mathbb{T}_N$  is the concatenation of  $N$  objects from  $\mathbb{T}$ , and we define it as  $T = (t_1, \dots, t_N)$ , with  $t_k \in \mathbb{T}$ . When we apply the tuple  $T$  to a datapoint  $x$ , we apply all the transformations from  $t_1$  to  $t_N$ . Armed with this set, we propose the following combinatorial optimization problem

$$\min_{T^* \in \mathbb{T}_N} f(\mathbb{M}, T^*, D) \quad (2)$$

where  $f$  is a fitness function that, fixed a model  $\mathbb{M}$  and a set of labelled datapoints  $D$ , measures the accuracy obtained when applying a transformation tuple  $T^*$  to the latter. Assuming that the maximum and minimum values for the accuracy are 1 and 0, respectively,  $f$  provides the mapping

$$f : T \longrightarrow [0, 1] \subset \mathbb{R}^1$$

Intuitively, the  $N$ -tuples that induce lower  $f$  values, are the ones that a model  $\mathbb{M}$  is more vulnerable to, with respect to the chosen metric. For classifiers, the optimization problem 2 assumes the form

$$\min_{T^* \in \mathbb{T}_N} f := \frac{1}{m} \sum_{i=0}^m \mathbb{1}\{y^{(i)} = \mathbb{M}(T^*(x^{(i)}))\} \quad (3)$$

In general, one can define an instance of problem 2 if provided with a set of annotated samples  $D$ , a transformation set  $\mathbb{T}$  (and, consequently, a tuple set  $\mathbb{T}_N$ ), a model  $\mathbb{M}$ , a measure to evaluate the performance of the model, and, consequently, a fitness function  $f$ . It is not required to have access to the model parameters: it can be a black-box.

A legit critique to this problem formulation is that we are not constraining the transformation tuples to be content-preserving. For instance, in the classification problem 3, the correct formulation would include a constraint similar to the following:

$$\mathcal{O}(x^{(i)}) = \mathcal{O}(T^*(x^{(i)})) \quad \forall i,$$

which means that an oracle  $\mathcal{O}(\cdot)$  would classify the transformed images in the same way as the original images. In this work, we do not explicitly constraint the transformation tuples to be content-preserving through the optimization problem. We satisfy the constraint by properly defining the set of available content-preserving image-transformations, *e.g.*, focusing on simple color transformations such as RGB enhancements or contrast/brightness adjustments, and setting a proper value for  $N$  in  $\mathbb{T}_N$ . Explic-

<sup>2</sup>To provide a practical example, one object from  $\mathbb{T}$  might be the “contrast” operation, and the intensity level might be +6%.

---

### Algorithm 1 RS (Random Search)

---

- 1: **Input:**  $N$ -tuple set  $\mathbb{T}_N$ , model  $\mathbb{M}$ , dataset  $D = \{(x^{(i)}, y^{(i)})\}_{i=1}^n$ , fitness function  $f$ .
  - 2: **Output:** transformation  $T \in \mathbb{T}_N$
  - 3: **Initialize:**  $f_{min} \leftarrow 1$ .
  - 4: **for**  $k = 1, \dots, K$  **do**
  - 5:     Sample  $T^*$  uniformly from  $\mathbb{T}_N$
  - 6:      $f^* \leftarrow f(\mathbb{M}, T^*, D)$
  - 7:     **if**  $f^* < f_{min}$  **then**
  - 8:          $T \leftarrow T^*$
- 

itly imposing the constraint is an interesting research direction, since it would allow to consider more complex sets, and we reserve it for future work.

## 2.1. Transformation set and size of the search space

Given a transformation set  $\mathbb{T}$  with  $N_T$  available transformations  $\tau_k$ , where the  $k_{th}$  has  $N_k$  available magnitude values, the size of  $\mathbb{T}_N$ , and consequently the size of the search space of the optimization problem 2, is  $S = (\sum_{t=0}^{N_T} N_t)^N$ .

In this work, we consider a transformation set  $\mathbb{T}$  which includes standard image transformations from the Python library Pillow [4], as done by Cubuk et al. [13], and a few more we included. It is defined by the following transformations, with the number of available intensity levels indicated in parenthesis: *autocontrast* (20), *sharpness* (20), *brightness* (20), *color* (20), *contrast* (20), *grayscale conversion* (1), *R-channel enhancer* (30), *G-channel enhancer* (30), *B-channel enhancer* (30), *solarize* (20).

This set results in a search space with size  $S = 211^N$ . Throughout this work, we will consider tuple sets  $\mathbb{T}_N$  with  $N = 3$  and  $N = 5$ , resulting in search spaces of size  $S \simeq 10^6$  and  $S \simeq 10^{12}$ , respectively. We refer to [3, 2] for a proper description of the different transformations. The *R/G/B-channel enhancement* operations simply add a bias to the RGB pixel values. We will describe the different ranges of intensity levels for each experiment (Table 2).

## 3. Searching worst-case image transformations

In this section, we analyze different solutions to face the combinatorial optimization problem 2. Specifically, the two approaches rely on random search and evolution-based [37] search. We provide a proof of concept experiment on MNIST models, and report a more exhaustive experimental evaluation in Section 5.

### 3.1. Random search.

Facing the combinatorial optimization problem 2 through random search is important for several reasons. First of all, it is the simplest approach that we can adopt, and thus it is worth to be explored. Further, it is often

a very strong baseline to compare against, as shown, *e.g.*, in hyper-parameter optimization [8] and neural architecture search [32]. Finally, it sheds light on the following question: *how is a model affected by random image transformations?*

The idea is to evaluate the fitness function  $f$  over an arbitrary number of random transformation tuples, thus the implementation is straightforward. For clarity and reproducibility, we detail it step-by-step through Algorithm 1. In the following, we will refer to this procedure as RS (short for Random Search)

### 3.2. Evolution-based search.

We define a simple evolution-based algorithm [37], aimed at minimizing the objective in problem 2. Each individual of the population is defined by a transformation  $N$ -tuple from a set  $\mathbb{T}_N$ . We define standard *Selection*, *Crossover* and *Mutation* operations. For a detailed explanation of genetic algorithms and the definitions we provided, we refer to [37]. In the following, we briefly discuss how we use these concepts in our framework.

- **Selection.** Given in input a population  $\text{pop} = \{T^p\}_{p=1}^P$ , the fitness score of each individual  $\text{fit} = \{f^p\}_{p=1}^P$ , and a positive integer  $n$ , returns in output a population of  $n$  individuals sampled from  $\text{pop}$  with weights proportional to  $\frac{1}{f^p}$ .
- **Crossover.** Given in input two initialized populations  $\text{pop1} = \{T^p\}_{p=1}^P$ , where  $T^p = (t_1^p, \dots, t_N^p)$  and  $\text{pop2} = \{\tilde{T}^p\}_{p=1}^P$ , where  $\tilde{T}^p = (\tilde{t}_1^p, \dots, \tilde{t}_N^p)$ , for each couple of elements  $\{(T^p, \tilde{T}^p)\}_{p=1}^P$ , it uniformly draws an integer  $m \in [1, m]$  and return the following two individuals:  $T^{p,1} = (t_1^p, \dots, t_m^p, \tilde{t}_{m+1}^p, \dots, \tilde{t}_N^p)$  and  $T^{p,2} = (\tilde{t}_1^p, \dots, \tilde{t}_m^p, t_{m+1}^p, \dots, t_N^p)$ . If the size of  $\text{pop1}$  and  $\text{pop2}$  is  $P$ , the new population will thus have  $2P$  individuals.
- **Mutation.** Given in input an initialized population  $\text{pop1} = \{T^p\}_{p=1}^P$  and a mutation rate  $\eta$ , it changes each transformation of each tuple in  $\text{pop}$  with probability  $\eta$ , sampling from  $\mathbb{T}$ .

Endowed of these methods, we implement an evolution-based search procedure, detailed in Algorithm 2. The asymptotic computational complexity is  $\mathcal{O}(PK)$ , where  $P$  is the population size and  $K$  is the number of evolutionary steps. Notice that the operations associated with lines 5 and 11, namely computing the fitness function value for each transformation in the population, constitute the computationally expensive part of the algorithm. For each run, we perform  $P(K + 1)$  fitness function evaluations. In the following, we will refer to this procedure as ES (short for Evolution-based Search).

---

### Algorithm 2 ES (Evolution-based Search)

---

- 1: **Input:**  $N$ -tuple set  $\mathbb{T}_N$ , model  $\mathbb{M}$ , dataset  $D = \{(x^{(i)}, y^{(i)})\}_{i=1}^n$ , fitness function  $f$ , population size  $P$ , mutation rate  $\eta$ .
  - 2: **Output:** transformation  $T \in \mathbb{T}_N$
  - 3: **Initialize:**  $f_{min} \leftarrow 1$ .
  - 4:  $\text{pop} \leftarrow \{T^p\}_{p=1}^P$  sampling from  $\mathbb{T}_N$
  - 5:  $\text{fit} \leftarrow \{f^p \leftarrow f(\mathbb{M}, T^p, D)\}_{p=1}^P$
  - 6: **for**  $k = 1, \dots, K$  **do**
  - 7:    $\text{newgen1} \leftarrow \text{Select}(\text{pop}, \text{fit}, \frac{P}{2})$
  - 8:    $\text{newgen2} \leftarrow \text{Select}(\text{pop}, \text{fit}, \frac{P}{2})$
  - 9:    $\text{pop} \leftarrow \text{Crossover}(\text{newgen1}, \text{newgen2})$
  - 10:    $\text{pop} \leftarrow \text{Mutation}(\text{pop}, \eta)$
  - 11:   Update  $\text{fit}$  as in line 5
  - 12:   **for**  $p = 1, \dots, P$  **do**
  - 13:     **if**  $\text{fit}[p] < f_{min}$  **then**
  - 14:        $T \leftarrow \text{pop}[p]$
- 

### 3.3. Proof of concept: MNIST

The MNIST dataset [28] is defined by  $28 \times 28$  pixel images, representing white digits on a black background. It is divided on a 50,000 sample training set and a 10,000 sample test set. In our experiments, we train a small ConvNet (*conv-pool-conv-pool-fc-fc-softmax*) on the whole training set. We resize the images to  $32 \times 32$  pixels, in order to be comparable with other digit datasets (in view of the domain generalization experiments reported in Section 5). We apply the search algorithms (RS and ES) on problem 2 using 1,000 samples from the test set. We set  $N = 3$ , namely, we use transformation tuples defined by three transformations.

The blue curve in Figure 2 is the density plot associated with all the fitness function values obtained while running RS for  $K = 10,000$  iterations, using as model  $\mathbb{M}$  a trained ConvNet that achieves 99.3% accuracy on the clean test set. The accuracy values are reported on the x-axis. Values lower than the one indicated by the black flag have less than 0.1% probability to be achieved by transforming the input through transformation tuples sampled from  $\mathbb{T}_N$ . This plot provides a useful glance on the vulnerability of MNIST models to random image transformations included in our set. It shows that there is a substantial mass of transformation tuples that the model is resistant to, but, even though with lower probability to be sampled, there are transformation tuples against which the model is severely vulnerable.

Table 1 (RS row) shows the minimum accuracy obtained in 10,000 evaluations of the fitness function  $f$ , averaged over 6 different models. We report results associated with both models trained via standard ERM (homonymous column) and models trained through the method proposed in [53] (“ADA” column). As one can observe, both types of models are severely vulnerable to the transformation tuples



Performance of MNIST models

Test	Training procedure				
	ERM	ADA [53]	RDA	RSDA	ESDA
Original	.993 ± .001	.992 ± .001	.993 ± .001	.992 ± .001	.993 ± .001
RS	.160 ± .024	.192 ± .025	.941 ± .011	.977 ± .001	.979 ± .003
ES	.122 ± .028	.177 ± .042	.927 ± .007	.979 ± .005	.977 ± .000
Neg. [22]	.436 ± .042	.448 ± .046	.991 ± .001	.992 ± .001	.992 ± .001
SAE [23]	.979 ± .005	.980 ± .005	.985 ± .004	.974 ± .007	.971 ± .016

Table 1. Accuracy values associated with MNIST models in different training/testing conditions, averaged over 6 different training runs. Each row is associated with a different test: *Original* refers to results obtained on original test samples; RS and ES refer to results obtained applying the transformations found via RS and ES, respectively; Neg and SAE are related to adversarial attacks detailed in [22] and [23], respectively. Each column is related to models trained with a different procedure. See details in the text.

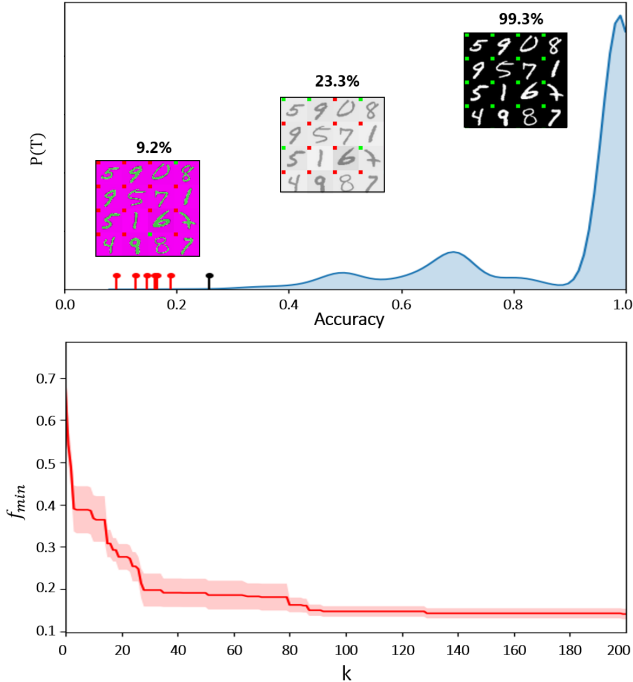


Figure 2. *Top*. The blue curve represents the density plot of the accuracy values  $f$  obtained via 10,000 transformation tuples found via RS. The black flag represents the 0.1% probability threshold in RS. The red flags represent the accuracy values obtained via ES. Three sample sets resulting from different transformations are reported, with green and red squares indicating whether the sample is mis-classified or not, respectively. *Bottom*.  $f_{min}$  values averaged over 6 runs of ES.

found through RS. For comparison with previous work, we also report results obtained on negative images [22] and on images with random hue/value perturbations [23] (for the latter we used the original code).

We proceed by approaching problem 2 through ES, setting population size  $P = 10$ , number of generations  $K = 99$  and mutation rate  $\eta = 0.1$ . With this setting, the number of fitness evaluations is 1,000. The red flags in Figure 2 indicate the  $f_{min}$  values achieved on 6 different runs, using

### Algorithm 3 Robust Training

- 1: **Input:**  $D = \{(x^{(i)}, y^{(i)})\}_{i=1}^n$ , initialized weights  $\theta_0$ ,  $N$ -tuple set  $\mathbb{T}_N$ , initialized data augmentation set  $\mathbb{T}_{tr}$ , learning rate  $\alpha$ .
- 2: **Output:** learned weights  $\theta$
- 3: **Initialize:**  $\theta \leftarrow \theta_0$
- 4: **for**  $h = 1, \dots, H$  **do**
- 5:     **for**  $j = 1, \dots, J$  **do**
- 6:         Sample  $(x, y)$  uniformly from  $D$
- 7:         Sample  $T$  uniformly from  $\mathbb{T}_{tr}$
- 8:          $\theta \leftarrow \theta - \alpha \nabla_{\theta} \ell(\theta; (T(x), y))$
- 9:         Find  $T^* \in \mathbb{T}_N$  by running RS or ES on a subset of  $D$
- 10:         Append  $T^*$  to  $\mathbb{T}_{tr}$
- 11:     **while** training is not done **do**
- 12:         Sample  $(x, y)$  uniformly from dataset
- 13:         Sample  $T$  uniformly from  $\mathbb{T}_{tr}$
- 14:          $\theta \leftarrow \theta - \alpha \nabla_{\theta} \ell(\theta; (T(x), y))$

the same ConvNet as in the RS experiment. A comparison between the 0.1% threshold (black flag) and the results obtained via evolution shows that ES allows to efficiently find low-probability transformation tuples that the model is most vulnerable to. Furthermore, even though we set  $K = 99$ , EF can find transformation tuples that go beyond the 0.1% threshold in less iterations. We report this evidence in Figure 2 (bottom), which shows the evolution of  $f_{min}$  during 200 iterations of ES. Comparing this result with the ones pictured in Figure 2 (top), one can observe that even by setting  $K \simeq 30$  ( $\sim 310$  fitness function evaluations), ES outperforms the 0.1% threshold in the RS results. We report numerical results in Table 1 (ES row), where we average over 6 models the lowest  $f_{min}$  achieved over 6 runs of ES with different initializations. In Section 5, we will provide a more exhaustive analysis of the efficacy of RS and ES to approach different instances of problem 2.

## 4. Training more robust models

In this section, we detail two straightforward methods devised to train models which are robust against content-preserving transformations from a given set.

The simplest approach that one can devise is likely the following: given a set  $\mathbb{T}_N$ , we can perform data augmentation by sampling transformation tuples  $T \in \mathbb{T}_N$  and applying them to the training images throughout the training procedure. We term this method *Randomized Data Augmentation*, in short RDA. This technique can be interpreted as an application of domain randomization [49] to real data instead of simulated ones.

Drawing inspiration from the literature related to adversarial robustness [18, 47, 53], where a loss is minimized with respect to inputs that are adversarial for the current

Transformation Sets $\mathbb{T}$ for the Experiments						
Transformations	Range	No. Levels	Experiment			
			MNIST [28]	CIFAR-10 [27]	CamVid [10]	Faces [1]
<i>Autocontrast</i>	[0.0, 0.3]	20	✓	✓	✓	✓
<i>Brightness</i>	[0.6, 1.4]	20	✓			
	[0.8, 1.2]	20		✓	✓	✓
<i>Color</i>	[0.6, 1.4]	20	✓	✓	✓	✓
<i>Contrast</i>	[0.6, 1.4]	20	✓	✓	✓	✓
<i>Sharpness</i>	[0.6, 1.4]	20	✓	✓	✓	✓
<i>Solarize</i>	[0.0, 20.0]	20	✓			
<i>Grayscale</i>	–	1	✓			✓
<i>R-channel enhancer</i>	[−120, 120]	30	✓		✓	✓
	[−30, 30]	30		✓		
<i>G-channel enhancer</i>	[−120, 120]	30	✓		✓	✓
	[−30, 30]	30		✓		
<i>B-channel enhancer</i>	[−120, 120]	30	✓		✓	✓
	[−30, 30]	30		✓		
<b>Size of <math>\mathbb{T}_N</math></b>			$211^N$	$190^N$	$190^N$	$191^N$

Table 2. List of the transformations used (column 1), with the range of magnitude values (columns 2) and the number of values in which the ranges have been discretized (column 3). Columns 4 – 7 indicate with ✓ whether a transformation is used in the experiments of Sections 5.1, 5.2, 5.3 and 5.4, respectively. Grayscale conversion (*Grayscale*) does not require a magnitude value. For all the transformations excluding *R/G/B-channel enhancement* operations, we refer to the PIL library [4] documentation, in particular to [3, 2]. In *R/G/B-enhancement*, we simply add/subtract a value determined by the magnitude level to the associated channel.

model, we devise a different method, more effective than RDA in our setting. We propose a training procedure where transformation tuples that the current model is most vulnerable to are searched throughout the training procedure (via RS or ES), and data augmentation is performed accordingly to the so-found transformations. We implement this idea as follows: (a) we define a transformation set to sample from during training (the “data augmentation set”  $\mathbb{T}_{tr}$ ), that at the beginning of training only comprises the *identity* transformation; (b) we train the network via gradient descent updates, augmenting samples via transformations uniformly sampled from  $\mathbb{T}_{tr}$  (in this work, the loss  $\ell$  used is the cross-entropy function between the output of the model and the ground truth labels); (c) we run RS or ES, using appropriate fitness function  $f$  and tuple set  $\mathbb{T}_N$ , and append the so-found transformation to  $\mathbb{T}_{tr}$ . We alternate between steps (a) and (b) for the desired number of times. (d) We repeat (a) until the value of the loss  $\ell$  is satisfactory.

The procedure is also detailed in Algorithm 3. As results will show, in several settings the latter method performs substantially better than RDA. In the next Sections, we will refer to this method as RSDA or ESDA, short for *Random Search Data Augmentation* and *Evolution-based Search Data Augmentation*, respectively

## 5. Experiments

We provided in Section 3.3 a first evidence that the problem described in Section 2 can be useful to detect distributional shifts, in terms of transformation tuples against which a model is most vulnerable. In Section 4, we introduced different methods to train more robust models.

In this section, we further validate the effectiveness of RS and ES on different instances of problem 2, associated with models for classification, semantic segmentation and face detection. Furthermore, we evaluate the performance of classification and semantic segmentation models trained through RDA, RSDA and ESDA, evaluating both the robustness against image transformations and the domain generalization properties. When we search for transformations while running RSDA and ESDA (Algorithm 3, line 9), we set  $K = 100$  for RS and  $K = 10$  for ES. When we apply ES, we set number of individual  $P = 10$  and mutation rate  $\eta = 0.1$  throughout the entire analysis. Table 2 reports the transformation set  $\mathbb{T}$  used in every experiments. We use accuracy as evaluation metric in all the experiments.

### 5.1. Digit Recognition

**Experimental setup.** We adopt the same experimental setting detailed in Section 3.3. We train models via ERM and RDA for  $10^6$  gradient descent updates. When we train models through RSDA/ESDA, we set  $J = 10^4$  and

Domain generalization performance of MNIST models				
Training Method	Testing dataset			
	SVHN	SYN	MNIST-M	USPS
ERM	.365 ± .021	.477 ± .015	.590 ± .012	.812 ± .013
ADA [53]	.391 ± .017	.482 ± .019	.595 ± .013	.819 ± .016
RDA	.395 ± .017	.603 ± .005	.751 ± .013	.832 ± .013
RSDA	.474 ± .048	.620 ± .012	.815 ± .016	.831 ± .012
ESDA	.489 ± .052	.622 ± .013	.816 ± .016	.840 ± .012

Table 3. Performance of MNIST models trained with different methods (rows) and evaluated on test samples from different digit datasets (columns). Results obtained by averaging over 3 different runs.

$H = 100$ , running a total of  $10^6$  weight updates also in this case. We use a subset of 1,000 samples from the training set when we run RS/ES (Algorithm 3, line 9). In all experiments, we set the size of the transformation tuples as  $N = 3$ . We use Adam [26] with learning rate  $\alpha = 3 \cdot 10^{-4}$ .

In addition to testing model vulnerability against transformations found via RS and ES, we also evaluate the generalization capabilities of MNIST models, testing on different, unseen digit datasets (SVHN [42], SYN [15], MNIST-M [15], USPS [14]), following the evaluation protocol proposed in [53]. Samples from every dataset were resized to  $32 \times 32$  pixels and treated as RGB images, to be comparable. Notice that we do not use samples from other dataset than MNIST until the testing phase (which is the difference between domain *generalization* and *adaptation* setups).

**Results.** In Section 3.3 we showed that our setup allows to find transformation tuples that lower the accuracy of MNIST models as low as  $\sim 12\%$  (Table 1 – row ES, column ERM). We are now interested in evaluating the performance on MNIST models trained through the methods detailed in Section 4 (RDA, RSDA and ESDA). Table 1 (last three columns) shows the performance of models trained with the proposed methods. The most robust model is the one trained through ESDA, for which the accuracy related to each testing case is  $> 97\%$ . All our models are resistant to the negative operation applied to the images [22] (accuracy  $> 99\%$ ). An important result to highlight, is that there is not a statistically significant accuracy loss on original samples (Table 1 – first row).

Having confirmed that we can train more robust models against the types of transformations introduced in this work, we are interested in evaluating the performance achieved in unseen domains. Table 3 reports our findings. Also in this experiment, we confirm that models trained via ESDA are the most robust against distributional shifts. Models trained via RSDA are slightly less performing, but significantly more robust than the ones trained via RDA in different test cases. The more significant result is that, when test-

ing on SVHN, there is  $\sim 10\%$  gap when comparing RDA and ESDA. Curiously, despite our transformation set  $\mathbb{T}$  is biased towards color transformations, we can observe improved performance with respect to ERM also when testing on USPS, whose samples differ from MNIST ones only in their shape.

## 5.2. CIFAR-10 Classification

**Experimental setup.** We use the CIFAR-10 [27] dataset, and train Wide Residual Network models (WRN [54]) on the training set. We have chosen this class of models because they are broadly used in the community and they provide results competitive with the state of the art on CIFAR-10. We train networks with 16-layers and set the width to 4, choosing a trade-off between accuracy and training/testing speed, among the recipes proposed in the original work [54]. We use the original code provided by the authors [5]. For training the models, we follow the procedure proposed in [5], and run SGD with momentum 0.9 for 200 epochs, starting with a learning rate 0.1 and decaying it at epochs 60, 120 and 160.

We observe that, in this particular setting, both RSDA and ESDA perform better if the new augmentation rules are included while we are training the model with a large learning rate. For this reason, we start the learning rate decay after having searched for a satisfactory number of transformations. In the results proposed in this section, we search for 100 different ones, and each search procedure is followed by 5 epochs of training. When we search for transformations, we use 2,000 samples drawn from the training set. We set the size of the tuples in  $\mathbb{T}_N$  as  $N = 5$ .

When we test the models, we search for transformations through RS and ES using the whole test set. We run RS with  $K = 1,000$  iterations and three runs of ES with  $K = 100$  iterations. The results reported in the next paragraph are associated with the optimal  $f_{min}$  found. In addition to testing the model vulnerability against such transformations, we also evaluate the generalization capabilities of WRN models, evaluating the performance on CIFAR-10.1 [43] dataset and on STL [12] dataset. We remove samples associated with the class “monkey”, not present in the CIFAR-10 dataset, and resize images to  $32 \times 32$ , to be comparable.

**Results.** Table 4 reports the results we achieved. The “ERM” column, showing results obtained by testing baseline models in different conditions, confirms the results we observed in the MNIST experiment, although with less dramatic effects. Indeed, while we obtain WRN accuracy close to 95%, we can find transformations that the model is significantly vulnerable to by using RS ( $\sim 72\%$ ) and ES ( $\sim 56\%$ , with a larger standard deviation). Concerning models trained with our methods, also in this experiment RDA is an effective strategy, but RSDA and ESDA allow

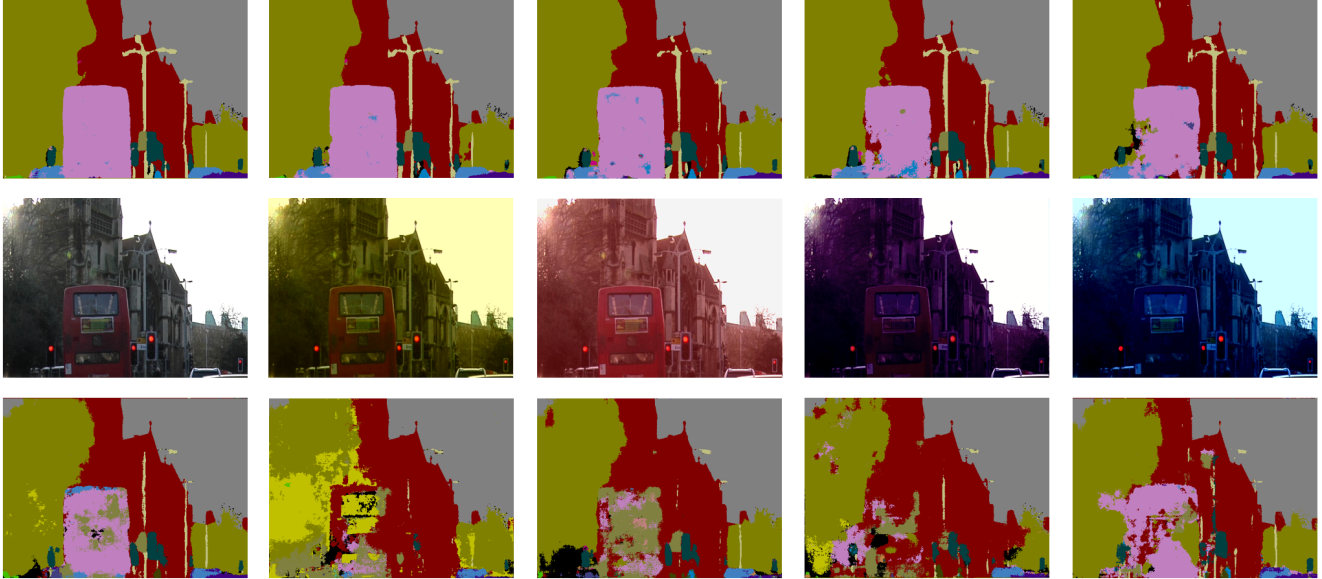


Figure 3. A sample from CamVid (column 1, row 2) modified with image transformations found via RS and ES (columns 2 – 5, row 2). Rows 1 and 3 report the output of a model train through the ESDA algorithm and a model trained via standard ERM, respectively.

Performance of CIFAR-10 models				
Test	Training procedure			
	ERM	RDA	RSDA	ESDA
Original	.946 ± .000	.944 ± .002	.950 ± .002	.946 ± .000
RS	.724 ± .026	.899 ± .004	.904 ± .016	.915 ± .000
ES	.565 ± .149	.862 ± .012	.867 ± .050	.913 ± .004
10.1 [43]	.872 ± .004	.873 ± .007	.886 ± .009	.878 ± .003
STL [12]	.466 ± .009	.503 ± .009	.526 ± .007	.534 ± .009

Table 4. Performance of CIFAR-10 models trained with different methods (columns) and tested in different conditions (rows). Row 10.1 reports results obtained by testing on CIFAR-10.1 [43], Row STL the ones related to STL [12]. Results obtained by averaging over 3 different runs.

to train more robust models, with respect to the transformations we are testing against.

Furthermore, the last row, reporting the results obtained when testing on STL dataset, confirms the domain generalization capabilities of models trained with our method: using the ESDA algorithm, we can observe  $\sim 7\%$  improvement in accuracy, when compared against ERM. When testing on CIFAR 10.1, the benefits are less marked. Each result proposed was obtained by averaging over accuracy values obtained in three different runs.

### 5.3. Semantic Scene Segmentation

**Experimental setup.** We train FC-DenseNet [25] models on the CamVid [10] dataset. We use the 103-layer version of the model, relying on an open-source implementation [6]. Also in this case, the choice of the model is due to its success with respect to the analyzed benchmark. The CamVid

Performance of CamVid models				
Test	Training procedure			
	ERM	RDA	RSDA	ESDA
Original	.862 ± .007	.851 ± .004	.854 ± .003	.851 ± .002
RS	.458 ± .027	.812 ± .007	.825 ± .009	.820 ± .007
ES	.311 ± .013	.811 ± .011	.824 ± .008	.822 ± .008

Table 5. Performance of CamVid models trained with different methods (columns) and tested in different conditions (rows). Results obtained by averaging over 3 different runs.

dataset contains 367 training images, 101 validation images and 233 testing images from 32 classes. We lower the sample resolution from  $960 \times 720$  to  $480 \times 360$ , and train the models for 300 epochs.

When we train using RSDA/ESDA, we run RS and ES on 30 samples from the training set, and search for new transformations every 10 epochs. We set the size of the  $N$ -tuples as  $N = 5$ . When we test the vulnerability of the models, we run RS (with  $K = 500$ ) and three different runs of ES (with  $K = 50$ ) on 30 samples from the test set. As for previous experiments, we report results related to the minimum  $f_{min}$  values found. Notice that the output of semantic segmentation models is richer than the output of classification models, since a prediction is associated with each pixel; indeed, 30 test samples lead to  $30 \cdot 480 \cdot 960$  pixel predictions. We use pixel accuracy as a metric [34].

**Results.** Table 5 reports the results we obtained. They confirm the higher level of robustness of models trained via RDA, RSDA and ESDA. In this experiment though, we can



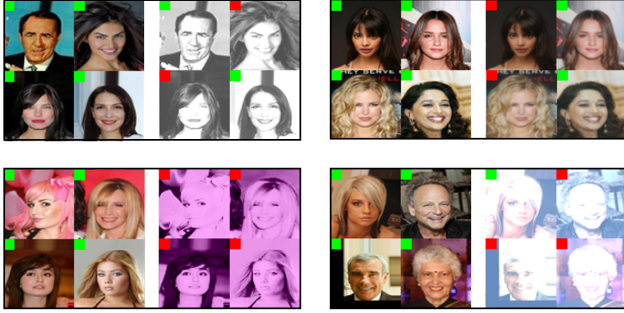


Figure 4. Four different examples of transformations found via RS and ES. Green and red squares indicate whether the API has detected the face or not, respectively.

Performance of Face Detection API [1]

Original Accuracy	RS N=3	ES N=3	RS N=5	ES N=5
$.878 \pm .007$	$.789 \pm .010$	$.705 \pm .069$	$.516 \pm .014$	$.174 \pm .134$

Table 6. Accuracy of the Face Detection API in different testing conditions, analogously to the previous tests reported in this work.

observe a narrower gap between RDA and RSDA/ESDA.

Figure 3 shows the output of the model trained via ESDA (top) and the output of a model trained via standard ERM (bottom), when the original input (first column) is perturbed by different image transformations (middle). These results not only qualitatively show the better performance of ESDA, but also that the transformation tuples we are sampling from  $\mathbb{T}_N$  are realistic approximations of possible visual conditions that a vision module (for instance, for a self-driving car) might encounter. Please note, for example, images in the middle row, second and third column, which can be considered as simulations of the light that one could encounter during dawn or sunset – and in which the baseline model performs poorly.

#### 5.4. Face detection

**Experimental setup.** We test our search methods on a widely used API for face detection [1], that takes RGB images as input and provides in output the locations of the faces in the image. We use four subsets of 1,000 images uniformly sampled from the MS-Celeb-1M dataset [19], resized to  $64 \times 64$ , as input to RS and ES. Each image contains one face, thus the API gives in output a single location if it detects a face, or nothing otherwise. In practical terms, due to the nature of the input, we can interpret the API as a binary model and test it through the optimization problem 3. We set the number of transformations as  $N = 3$  and  $N = 5$ . For each  $N$  value and each subset of faces, we run RS with  $K = 15,000$  iterations, and run 6 different runs of ES with  $K = 100$ . We average results over the optimal  $f_{min}$  values obtained in the four subsets.

**Results.** Table 6 reports the accuracy values obtained, and Figure 4 reports different examples of faces modified through the transformation tuples found through RS and ES. Green and red squares indicate whether the API has detected or not a face, respectively. Qualitatively, we observed that the model tends to fail when the input manipulation is such that some facial features are no longer visible or deteriorated (for example, the nose). The importance of these vulnerabilities depends on the different API use cases. For example, vulnerability to some grayscale tones might not matter for a model that deals with images recorded in the streets, but it might matter for a social network application. Vulnerability to extreme brightness conditions can be harmful for a street camera, where the broad variety of possible visual conditions might not allow to have a proper view of the facial features. One strength of the search methods we proposed is that they allow users to set transformation sets accordingly to the applications they are concerned about.

## 6. Conclusions

We propose a combinatorial optimization problem to find distributional shifts that a given model is vulnerable to, in terms of  $N$ -tuples of image transformations. We show that random search and, in particular, evolution-based search are effective approaches to face this problem. Further, we show that the same search algorithms can be exploited in a training procedure, where harmful distributional shifts are searched and harnessed. We report results for a variety of tasks (classification, segmentation, face detection), showing that the problem formulation is flexible and can be adopted in different circumstances.

There are several possible directions for future works. First, the definition of a proper content-preserving constraint in the optimization problem would allow to consider more complex image transformation sets, as well as using  $N$ -tuples with larger  $N$  values without the risk of erasing the content of the image. Next, the implementation of more effective methods to approach the optimization problem 2, in order to find harmful transformations with reduced computational cost, is an important path to explore. Finally, in this work we limit the analysis to color transformations; an analysis of different transformation sets, including, *e.g.*, geometric transformations, would allow to learn models that generalize to a larger number of possible unseen distributions.

## Acknowledgments

We are grateful to Jacopo Cavazza and Federico Marmoreo for helpful discussions concerning the problem formulation proposed in this work.

## References

- [1] Face recognition. [https://github.com/ageitgey/face\\_recognition](https://github.com/ageitgey/face_recognition). 6, 9
- [2] Pillow imageenhance module. <https://pillow.readthedocs.io/en/3.0.x/reference/ImageEnhance.html>. 3, 6
- [3] Pillow imageops module. <https://pillow.readthedocs.io/en/3.0.x/reference/ImageOps.html>. 3, 6
- [4] Python imaging library. <https://github.com/python-pillow/Pillow>. 3, 6
- [5] Pytorch training code for wide residual networks. <https://github.com/szagoruyko/wide-residual-networks/tree/master/pytorch>. 7
- [6] Semantic segmentation suite. <https://github.com/GeorgeSeif/Semantic-Segmentation-Suite>. 8
- [7] S. Ben-David, J. Blitzer, K. Crammer, and F. Pereira. Analysis of representations for domain adaptation. In B. Schölkopf, J. C. Platt, and T. Hoffman, editors, *Advances in Neural Information Processing Systems 19*, pages 137–144. MIT Press, 2007. 1
- [8] J. Bergstra and Y. Bengio. Random search for hyperparameter optimization. *J. Mach. Learn. Res.*, 13:281–305, Feb. 2012. 4
- [9] J. Blitzer, R. McDonald, and F. Pereira. Domain adaptation with structural correspondence learning. In *Proceedings of the 2006 Conference on Empirical Methods in Natural Language Processing, EMNLP '06*, pages 120–128, Stroudsburg, PA, USA, 2006. Association for Computational Linguistics. 1, 2
- [10] G. J. Brostow, J. Shotton, J. Fauqueur, and R. Cipolla. Segmentation and recognition using structure from motion point clouds. In *ECCV (1)*, pages 44–57, 2008. 6, 8
- [11] T. Brown, D. Mane, A. Roy, M. Abadi, and J. Gilmer. Adversarial patch. 2017. 2
- [12] A. Coates, A. Ng, and H. Lee. An analysis of single-layer networks in unsupervised feature learning. In G. Gordon, D. Dunson, and M. Dudk, editors, *Proceedings of the Fourteenth International Conference on Artificial Intelligence and Statistics*, volume 15 of *Proceedings of Machine Learning Research*, pages 215–223, Fort Lauderdale, FL, USA, 11–13 Apr 2011. PMLR. 7, 8
- [13] E. D. Cubuk, B. Zoph, D. Mané, V. Vasudevan, and Q. V. Le. Autoaugment: Learning augmentation policies from data. *CoRR*, abs/1805.09501, 2018. 3
- [14] J. S. Denker, W. R. Gardner, H. P. Graf, D. Henderson, R. E. Howard, W. Hubbard, L. D. Jackel, H. S. Baird, and I. Guyon. Advances in neural information processing systems 1. chapter Neural Network Recognizer for Handwritten Zip Code Digits, pages 323–331. 1989. 7
- [15] Y. Ganin and V. S. Lempitsky. Unsupervised domain adaptation by backpropagation. In *Proceedings of the 32nd International Conference on Machine Learning, ICML 2015, Lille, France, 6-11 July 2015*, pages 1180–1189, 2015. 2, 7
- [16] R. Geirhos, P. Rubisch, C. Michaelis, M. Bethge, F. A. Wichmann, and W. Brendel. Imagenet-trained CNNs are biased towards texture; increasing shape bias improves accuracy and robustness. In *International Conference on Learning Representations*, 2019. 2
- [17] J. Gilmer, R. P. Adams, I. J. Goodfellow, D. Andersen, and G. E. Dahl. Motivating the rules of the game for adversarial example research. *CoRR*, abs/1807.06732, 2018. 1, 2
- [18] I. Goodfellow, J. Shlens, and C. Szegedy. Explaining and harnessing adversarial examples. In *International Conference on Learning Representations*, 2015. 2, 5
- [19] Y. Guo, L. Zhang, Y. Hu, X. He, and J. Gao. MS-Celeb-1M: A dataset and benchmark for large scale face recognition. In *European Conference on Computer Vision*. Springer, 2016. 9
- [20] C. Heinze-Deml and N. Meinshausen. Conditional variance penalties and domain shift robustness. *arXiv preprint arXiv:1710.11469*, 2017. 2
- [21] D. Hendrycks and T. Dietterich. Benchmarking neural network robustness to common corruptions and perturbations. In *International Conference on Learning Representations*, 2019. 2
- [22] H. Hosseini and R. Poovendran. Deep neural networks do not recognize negative images. *CoRR*, abs/1703.06857, 2017. 1, 2, 5, 7
- [23] H. Hosseini and R. Poovendran. Semantic adversarial examples. In *The IEEE Conference on Computer Vision and Pattern Recognition (CVPR) Workshops*, June 2018. 1, 2, 5
- [24] H. D. III and D. Marcu. Domain adaptation for statistical classifiers. *CoRR*, abs/1109.6341, 2011. 1, 2
- [25] S. Jegou, M. Drozdal, D. Vazquez, A. Romero, and Y. Bengio. The one hundred layers tiramisu: Fully convolutional densenets for semantic segmentation. *arXiv e-prints*, abs/1611.09326, 2016. 8
- [26] D. P. Kingma and J. Ba. Adam: A method for stochastic optimization. *CoRR*, abs/1412.6980, 2014. 7
- [27] A. Krizhevsky and G. Hinton. Learning multiple layers of features from tiny images. *Master's thesis, Department of Computer Science, University of Toronto*, 2009. 6, 7
- [28] Y. Lecun, L. Bottou, Y. Bengio, and P. Haffner. Gradient-based learning applied to document recognition. In *Proceedings of the IEEE*, pages 2278–2324, 1998. 2, 4, 6
- [29] J. Lee and M. Raginsky. Minimax statistical learning and domain adaptation with wasserstein distances. *arXiv preprint arXiv:1705.07815*, 2017. 2
- [30] D. Li, Y. Yang, Y. Song, and T. M. Hospedales. Deeper, broader and artier domain generalization. *The IEEE International Conference on Computer Vision (ICCV)*, 2017. 2
- [31] D. Li, J. Zhang, Y. Yang, C. Liu, Y. Song, and T. M. Hospedales. Episodic training for domain generalization. *CoRR*, abs/1902.00113, 2019. 2
- [32] L. Li and A. Talwalkar. Random search and reproducibility for neural architecture search. *CoRR*, abs/1902.07638, 2019. 4
- [33] Y. Li, Y. Yang, W. Zhou, and T. M. Hospedales. Feature-critic networks for heterogeneous domain generalization. *CoRR*, abs/1901.11448, 2019. 2
- [34] J. Long, E. Shelhamer, and T. Darrell. Fully convolutional networks for semantic segmentation. *CoRR*, abs/1411.4038, 2014. 8

- [35] A. Madry, A. Makelov, L. Schmidt, D. Tsipras, and A. Vladu. Towards deep learning models resistant to adversarial attacks. In *International Conference on Learning Representations*, 2018. [2](#)
- [36] M. Mancini, S. R. Bul, B. Caputo, and E. Ricci. Robust place categorization with deep domain generalization. *IEEE Robotics and Automation Letters*, 3(3):2093–2100, July 2018. [2](#)
- [37] M. Mitchell. *An Introduction to Genetic Algorithms*. MIT Press, Cambridge, MA, USA, 1998. [3](#), [4](#)
- [38] S.-M. Moosavi-Dezfooli, A. Fawzi, O. Fawzi, and P. Frossard. Universal adversarial perturbations. *2017 IEEE Conference on Computer Vision and Pattern Recognition (CVPR)*, pages 86–94, 2017. [2](#)
- [39] P. Morerio, J. Cavazza, and V. Murino. Minimal-entropy correlation alignment for unsupervised deep domain adaptation. *International Conference on Learning Representations*, 2018. [2](#)
- [40] S. Motiian, M. Piccirilli, D. A. Adjeroh, and G. Doretto. Unified deep supervised domain adaptation and generalization. In *The IEEE International Conference on Computer Vision (ICCV)*, Oct 2017. [2](#)
- [41] K. Muandet, D. Balduzzi, and B. Schölkopf. Domain generalization via invariant feature representation. In S. Dasgupta and D. McAllester, editors, *Proceedings of the 30th International Conference on Machine Learning*, volume 28 of *Proceedings of Machine Learning Research*, pages 10–18, Atlanta, Georgia, USA, 17–19 Jun 2013. PMLR. [2](#)
- [42] Y. Netzer, T. Wang, A. Coates, A. Bissacco, B. Wu, and A. Y. Ng. Reading digits in natural images with unsupervised feature learning. In *NIPS Workshop on Deep Learning and Unsupervised Feature Learning 2011*, 2011. [7](#)
- [43] B. Recht, R. Roelofs, L. Schmidt, and V. Shankar. Do CIFAR-10 classifiers generalize to cifar-10? *CoRR*, abs/1806.00451, 2018. [1](#), [7](#), [8](#)
- [44] B. Recht, R. Roelofs, L. Schmidt, and V. Shankar. Do imagenet classifiers generalize to imagenet? *CoRR*, abs/1902.10811, 2019. [1](#)
- [45] K. Saenko, B. Kulis, M. Fritz, and T. Darrell. Adapting visual category models to new domains. In *Proceedings of the 11th European Conference on Computer Vision: Part IV, ECCV’10*, pages 213–226, Berlin, Heidelberg, 2010. Springer-Verlag. [2](#)
- [46] S. Shankar, V. Piratla, S. Chakrabarti, S. Chaudhuri, P. Jyothi, and S. Sarawagi. Generalizing across domains via cross-gradient training. In *International Conference on Learning Representations*, 2018. [2](#)
- [47] A. Sinha, H. Namkoong, and J. Duchi. Certifiable distributional robustness with principled adversarial training. In *International Conference on Learning Representations*, 2018. [2](#), [5](#)
- [48] B. Sun and K. Saenko. Deep CORAL: correlation alignment for deep domain adaptation. In *Computer Vision - ECCV 2016 Workshops - Amsterdam, The Netherlands, October 8-10 and 15-16, 2016, Proceedings, Part III*, pages 443–450, 2016. [2](#)
- [49] J. Tobin, R. Fong, A. Ray, J. Schneider, W. Zaremba, and P. Abbeel. Domain randomization for transferring deep neural networks from simulation to the real world. *CoRR*, abs/1703.06907, 2017. [2](#), [5](#)
- [50] A. Torralba and A. A. Efros. Unbiased look at dataset bias. In *Proceedings of the 2011 IEEE Conference on Computer Vision and Pattern Recognition, CVPR ’11*, pages 1521–1528, Washington, DC, USA, 2011. IEEE Computer Society. [1](#)
- [51] E. Tzeng, J. Hoffman, K. Saenko, and T. Darrell. Adversarial discriminative domain adaptation. In *The IEEE Conference on Computer Vision and Pattern Recognition (CVPR)*, July 2017. [2](#)
- [52] R. Volpi, P. Morerio, S. Savarese, and V. Murino. Adversarial feature augmentation for unsupervised domain adaptation. In *The IEEE Conference on Computer Vision and Pattern Recognition (CVPR)*, June 2018. [2](#)
- [53] R. Volpi\*, H. Namkoong\*, O. Sener, J. Duchi, V. Murino, and S. Savarese. Generalizing to unseen domains via adversarial data augmentation. In *Advanced in Neural Information Processing Systems (NeurIPS) 32*, December 2018. [2](#), [4](#), [5](#), [7](#)
- [54] S. Zagoruyko and N. Komodakis. Wide residual networks. In *BMVC*, 2016. [7](#)